Application of Imaging Spectroscopy to Mapping Canopy Nitrogen in the Forests of the Central Appalachian Mountains Using Hyperion and AVIRIS

Philip A. Townsend, *Associate Member, IEEE*, Jane R. Foster, Robert A. Chastain, Jr., and William S. Currie

***Abstract*—Earth Observing 1 (EO-1) Hyperion and Airborne Visible/Infrared Imaging Spectrometer (AVIRIS) imagery were used to predict canopy nitrogen (N) concentration for mixed oak forests of Green Ridge State Forest in Maryland. Nitrogen concentration was estimated for 27 ground plots using leaf samples of the dominant tree species from each plot that were dried, ground and analyzed in the laboratory for foliar N concentration. Foliar N data were composited based on relative species composition to determine overall canopy N concentration for the plot. Hyperion and AVIRIS images were converted to surface reflectance and related to canopy N using partial least squares (PLS) regression of first-derivative reflectance for wavelengths reported in the literature to be associated with N absorption features. The PLS model for Hyperion employed four factors and accounted for 97.8% of the variation in N concentrations and 40.4% of the variation in the spectral data whereas the AVIRIS model used three factors accounting for 84.9% of the variation in N and 72.4% of the variation in the spectral information. In the area of overlap between the AVIRIS and Hyperion images, > 70% of the estimates from the two sensors were within 0.25%N of each other, indicating a very close fit between the models generated using data from Hyperion and AVIRIS. This research indicates the applicability of hyperspectral data in general and Hyperion data in particular for mapping canopy nitrogen concentration.**

***Index Terms*—Airborne Visible/Infrared Imaging Spectrometer (AVIRIS), Appalachian mountains, canopy nitrogen concentration, Hyperion, oak forests.**

I. Introduction

ONE OF THE GREAT promises of imaging spectroscopy (hyperspectral remote sensing) has been the potential for mapping nutrient concentrations in vegetation canopies [1]–[6]. Measurements of foliar biochemicals are important because they provide crucial information that allows the assessment of nutrient cycling, gas exchange, and plant productivity that are necessary for evaluating ecosystem functioning [7], [8]. Nitrogen in particular is an important indicator of photosynthetic and growth rates, and in areas such as the central Appalachian Mountains where atmospheric nitrogen deposition rates are high, the canopy N concentrations can indicate the potential for forests to utilize excess N for increased growth and carbon storage or alternately as a buffer against nitrogen saturation and leakage to surface waters [9]–[14]. Remote estimation provides the opportunity to make such measurements cost-effective over large areas.

The use of imaging spectroscopy to estimate foliar biochemical composition has been discussed extensively in the literature [1]–[8], [15]–[19], and is generally premised on the idea that radiance/reflectance spectra from vegetation canopies exhibit characteristic absorption features resulting from the vibration and bending of molecular organic bonds of carbon, nitrogen, hydrogen and oxygen within plants at shortwave infrared wavelengths and from electron transitions related to chlorophyll concentration in visible wavelengths [20], [21]. The objective of this paper is to test the capability of Hyperion, the imaging spectrometer aboard the Earth Observing 1 (EO-1) satellite, to map canopy nitrogen concentration for deciduous oak forests in the mountains of western Maryland, and to compare the results from those analyses with estimation made using the Airborne Visible/Infrared Imaging Spectrometer (AVIRIS).

Manuscript received July 20, 2002; revised January 12, 2003. This research was supported by the National Aeronautics and Space Administration Earth Observing 1 Science Validation Team under Grant NCC5–493.

The authors are with the University of Maryland Center for Environmental Science, Appalachian Laboratory, Frostburg, MD 21532 USA (e-mail: townsend@al.umces.edu).

Digital Object Identifier 10.1109/TGRS.2003.813205

II. Methods

A. Study Area

This study took place in a 25 000-ha region of the Green Ridge State Forest in western Maryland and adjacent Buchanan State Forest in Pennsylvania (Fig. 1). The area is located within the Ridge and Valley Province of the central Appalachian Mountains within an elevation range of 300–700 m. The vegetation is dominated by deciduous oaks in the canopy with varying understory species (Table I). The forests are even-aged (75–100 years) [22] and largely continuous with full-canopy closure despite modest variations in leaf area. The site is the location of several studies focusing on the effects of forest vertical structure on biodiversity as well as the consequences of repeated gypsy moth defoliation on ecosystem functioning and nutrient retention. A variety of remote sensing data as well as field measurements on forest structure (leaf area index, basal area, forest height), species composition, and ecosystem attributes (canopy and soil nutrients) were available from other studies (Table I). We used data from 27 existing plots for this research. Due to slight differences in Hyperion and AVIRIS coverage as well as cloud cover, 20 plots were used for the Hyperion analyses, 17

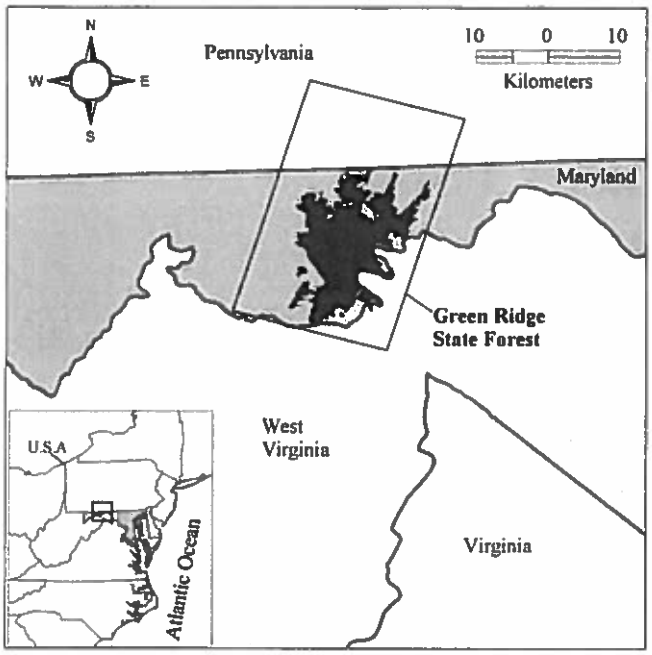

Fig. 1. Location of green ridge state forest, Maryland.

for AVIRIS, with ten plots included in both AVIRIS and Hyperion scenes (Table I).

B. Foliar Chemistry Data Collection and Analysis

All field plots had been previously sampled for species composition and forest structure. We used a variable-area sampling design suitable for integration with 30-m satellite data (described in detail in [23]; see also [24]), in which measurements of basal area by species, canopy cover by species and canopy heights (using a laser altimeter) were measured in an area slightly larger than 60 × 60 m. For this research, we collected green leaf samples from the central 30 × 30 m area of the plot between July 16–25, which was within 12 days of the AVIRIS overflight (July 13, 2001) and the Hyperion acquisition (July 24, 2001). At or near the time of leaf acquisition, we collected hemispherical photographs using a Nikon Coolpix digital camera (four to 20 per plot) that were analyzed using previously established procedures [25], [26] to determine the single-sided leaf area index (square meter per square meter) of the plot around the time of the image acquisition (Table I). Green leaf samples were collected using a shotgun from multiple trees per plot, usually two to three samples from all dominants or codominants and one sample from prominent subdominants and understory species. Leaf samples were composited by tree (following the general approach of [7]), dried to constant mass (70 °C), ground to #20 mesh in a Wiley Mill, stirred well, and subsampled (200 mg) for further grinding to #60 mesh. These were again dried to 70 °C and cooled in a laboratory desiccator until chemical analysis by dry combustion on a Carlo–Erba NC 2100 Analyzer. Sample sizes for analysis were approximately 10 mg. We performed dry weight corrections (105 °C) on all N concentration results using an empirical correction coefficient derived for similar forests in the central Appalachian region, and report the results here on a dry weight, ash-included basis. Total canopy N concentration for each field plot was estimated by weighting the foliar N estimate for each species on the plot by its relative basal area (Table I). For plots in which a species was present but not sampled, a regional mean for the species was employed (Table II). In the remainder of the paper, we report canopy N concentration as a percentage representing grams N per gram ash-included dry weight.

C. Remote Sensing Data

The Hyperion image was acquired by EO-1 on 24 July 2001, while the high altitude AVIRIS image was acquired on 13 July 2001 from the ER-2 aircraft flying at an altitude of 20 km. Hyperion has a spatial resolution of 30 m and covers a swath 256 pixels wide (7.68 km) × 180 km long. Hyperion measures 221 bands at approximately 10-nm intervals from 356–2577 nm. High altitude AVIRIS pixels have approximately 17–20-m spatial resolution and 224 bands at 10-nm intervals between 374–2508 nm. Green Ridge is covered by one AVIRIS flight line of 614 pixels (10.5) km. All image data were received with pixel values calibrated to radiance. For the Hyperion images, we developed a destriping algorithm in IDL to reduce the effects of random column-to-column noise in the spectral data resulting from the "pushbroom" (rather than "whiskbroom") design [27]. For each column in a band of the image, reflectance spectra were adjusted to make the column mean and variance match the image mean and variance [41]. Cloud/shadow and nonforest were masked for the generation of statistics during the destriping routine. For the AVIRIS image, we also applied an additional correction to reduce the effects of a cross-track view-angle dependent brightness gradient, also with cloud/shadow and nonforest masked. This gradient of increasing brightness on one side of the image results from the AVIRIS scan angle and direction, flight path orientation and solar azimuth, and was corrected by fitting a first-order additive quadratic curve to the mean radiance by view angle [28]. We used the atmospheric removal program of Gao *et al.* (Atmosphere Removal (ATREM) version 3.1) [29] to determine atmospheric water vapor content and then convert radiance values to ground reflectance estimates. Images were georeferenced using a triangulation method (AVIRIS) or second-order polynomials (Hyperion) and nearest neighbor resampling for > 70 ground control points per scene. Reflectance spectra were acquired for pixels within a radius of approximately 35 m around the center point of the field plots and averaged to estimate average reflectance for each field site. Analyses employed reflectance spectra (following [7]) although absorbance, calculated as $A = \log(1/R)$, has been used in numerous studies in the literature [21], [30].

D. Statistical Methods

We modeled canopy N concentration for a plot as an empirical function of image spectra. The independent variables were first-derivative reflectance spectra (as opposed to raw reflectance values), calculated for a given wavelength as the difference in smoothed reflectance (30-nm average) between bands 10 nm on either side of the given wavelength. The use of first-derivative spectra provided a surrogate for identifying the actual absorbance features that form the physical basis for

TABLE I
SPECIES COMPOSITION AND STAND INFORMATION FOR FIELD PLOTS USED IN THE RESEARCH

					Relative Importance of Dominant Species							
Plot ID	Sensors	Canopy N (%)	LAI (m^2m^{-2})	Basal Area (m^2ha^{-1})	White Oak	Red Oak	Chestnut Oak	Black Oak	Red Maple	Sugar Maple	White Pine	Virginia Pine
GR10150200	AVIRIS	2.12	2.81	36.8	15.2%	3.3%	44.6%	27.2%			1.1%	
GR1050100	AVIRIS	2.20	3.21	31.6	10.1%	1.3%	6.3%	5.1%	1.3%			20.3%
GR1050300	AVIRIS	2.40	3.35	30.4	11.8%	3.9%	30.3%	5.3%				21.1%
GR1150200	Both	2.29	1.80	21.2	3.8%	5.7%	22.6%			7.5%		1.9%
GR150100	Both*	2.48	3.18	29.6	2.7%	13.5%	36.5%	16.2%				1.4%
GR150300	Both	2.55	2.61	28.4	4.2%	18.3%	23.9%	18.3%		4.2%		
GR17150200	AVIRIS	2.27	2.83	28.4	29.6%	14.1%	11.3%	5.6%	5.6%	11.3%		1.4%
GR17200350	AVIRIS	2.46	3.29	23.2	25.9%	6.9%	22.4%	5.2%		15.5%		
GR1720050	AVIRIS	2.54	3.21	20.4	9.8%		19.6%	2.0%	2.0%	31.4%		
GR5150200	Both*	2.23	3.89	26.4	31.8%	3.0%	22.7%	7.6%	16.7%		1.5%	3.0%
GR5200350	Both*	2.44	3.25	19.2	12.5%	12.5%	4.2%	4.2%	29.2%	2.1%	8.3%	
GR520050	Both*	2.36	3.62	20.8	26.9%	9.6%	17.3%	5.8%	3.8%	11.5%		
GR8100250	Both	2.69	3.60	31.2	69.2%	12.8%			2.6%	11.5%	1.3%	
GR850100	Both	2.73	3.83	31.2	42.3%	11.5%			2.6%	20.5%	5.1%	
GR850400	Both	2.72	3.32	34.4	80.2%	9.3%				1.2%		
GYP1	Hyperion	2.38	2.47	25.9	0.0%	0.2%	53.4%	0.1%	3.0%		22.5%	16.0%
GYP10	Hyperion	2.35	2.24	12.7	11.7%	0.0%	36.1%	0.2%	36.2%	1.2%		
GYP11	Both	2.73	2.04	33.8	10.7%	32.8%	53.9%		0.0%			
GYP12	Hyperion	2.99	2.13	25.1	1.2%	21.1%	62.7%					4.0%
GYP2	Hyperion	2.65	2.58	34.9		5.9%	77.9%	14.5%	0.3%			
GYP3	Both	2.38	2.01	22.4	85.8%	0.0%	0.2%	6.7%				
GYP4	Hyperion	2.27	2.32	24.7	34.4%		12.4%	17.6%	1.2%			
GYP5	Hyperion	2.62	1.95	34.0	48.6%	30.0%	11.7%		0.2%			
GYP6	Both	3.07	2.78	22.5	2.7%	14.2%	65.9%	2.0%	7.9%	0.0%		
GYP7	Both	2.63	1.92	33.7			30.7%	47.5%	1.1%	2.9%		
GYP8	AVIRIS	2.69	2.61	33.0			29.9%	61.2%	3.2%			
GYP9	Both	2.63	2.50	24.6		24.2%	73.5%	0.2%	0.2%			

* Only used with Hyperion, exhibited cloud or shadow contamination on AVIRIS.

identifying foliar nutrient concentration through imaging spectroscopy. Specifically, the first-derivative identifies differences in the *slope* of the spectra, meaning that absorbance features related to canopy chemistry are identified through relative differences in the linear rate of change of reflectance within a given wavelength region. As a consequence, the actual bands identified as being related to N concentration may not in fact be centered on wavelengths known to exhibit absorbance features but rather those just adjacent to known absorbance features. We did not employ second-derivative spectra, although these have been suggested in the literature (see [30, Table IV]).

We employed partial least squares regression (PLS) to estimate canopy N concentration as a function of image measurement methods reported by several authors [6], [8], [31]. The benefit to using PLS for imaging spectroscopy applications is that it takes advantage of the high dimensionality of the spectral data by building predictive models through the extraction of factors (also called components or latent vectors) from the original data which best explain both the response and predictor variation [32]. In contrast, stepwise variable selection with ordinary least squares (OLS) regression is less preferred because of the potential for selecting wavelengths not associated with known absorption features (i.e., spurious correlations) [33]. PLS allows the use of either all spectral data or a selection of spectral wavelengths that have been reported to be related to N-absorption features.

For our implementation of PLS, we used first-derivative reflectance data from ±15 nm of the wavelength regions reported to be associated with known N absorbance features, as identified in a review of the literature. Curran *et al.* [5] noted key absorption bands associated with nitrogen bonds at 1020, 1510, 2060, 2130, 2180, and 2300 nm. Other sources also indicate the presence of absorption bands associated with nitrogen, proteins or amino acids at or near 1180–1200 nm, 1460 nm [20], 910 and 2350 nm [5]. Noise levels in the Hyperion images were considered too high to use wavelengths above 2300 nm. Some of the wavelengths noted in the literature (910 and 1180–1200 nm) have been identified as absorption features for proteins, though not specifically for nitrogen. However, because proteins are defined by the presence of an amino group ($-NH_2$), we included these wavelengths in the analysis. These bands were also used because many other wavelengths associated with N absorption features are located in regions of the electromagnetic spectrum (EMS) that are characterized by strong atmospheric water absorption features, rendering those wavelengths unusable in a remote sensing analysis. Finally, we chose to use one set of wavelengths from the visible-near infrared portion of the EMS. Although there are no absorption features directly associated with nitrogen in chemical bonds at the shorter wavelengths, wavelengths below 800 nm are strongly associated with other vegetation characteristics, especially vegetation greenness (as evidenced by chlorophyll concentrations and the differences in reflectance at NIR and red wavelengths). However, vegetation greenness represents a surrogate indicator of N levels (i.e., greener, more vigorous vegetation will have greater concentrations of N).

TABLE II
FOLIAR NITROGEN CONCENTRATION OF SPECIES SAMPLED IN THE STUDY

Scientific name	Common name	Trees sampled	Min N (%)	Max N (%)	Mean N (%)	Std Dev N (%)
Acer pensylvanicum	Striped maple	1	2.72	2.72	2.72	
Acer rubrum	Red maple	34	1.81	3.23	2.39	0.39
Acer saccharum	Sugar maple	9	1.99	2.84	2.47	0.29
Amelanchier arborea	Serviceberry	2	1.81	2.10	1.96	0.21
Betula lenta	Black birch	4	2.85	3.47	3.11	0.28
Carya alba	Mockernut hickory	1	2.27	2.27	2.27	
Carya glabra	Pignut hickory	6	2.10	4.24	2.55	0.84
Carya ovata	Shagbark hickory	2	2.80	2.88	2.84	0.06
Cornus florida	Flowering dogwood	1	2.41	2.41	2.41	
Fagus grandifolia	Beech	2	2.95	2.99	2.97	0.03
Fraxinus americana	White ash	2	2.29	2.30	2.30	0.01
Hamamelis virginiana	Witch-hazel	3	2.28	2.71	2.46	0.22
Kalmia latifolia	Mountain laurel	2	1.53	1.66	1.59	0.09
Lindera benzoin	Spicebush	1	4.07	4.07	4.07	
Liriodendron tulipifera	Tulip poplar	1	4.12	4.12	4.12	
Nyssa sylvatica	Black gum	3	2.52	2.71	2.60	0.10
Ostrya virginiana	Hop-hornbeam	1	2.23	2.23	2.23	
Prunus serotina	Pin cherry	1	3.70	3.70	3.70	
Quercus alba	White oak	38	1.67	3.38	2.49	0.41
Quercus coccinea	Scarlet oak	3	1.91	2.30	2.09	0.20
Quercus prinus	Chestnut oak	54	1.78	3.53	2.72	0.33
Quercus rubra	Red oak	54	2.10	3.85	2.87	0.35
Quercus velutina	Black oak	9	1.43	2.76	2.45	0.40
Rhododendron maximum	Rhododendron	1	1.23	1.23	1.23	
Tilia americana	Basswood	2	3.82	4.03	3.92	0.15
Vaccinium spp.	Blueberry	5	1.97	2.35	2.21	0.15

Therefore, we employed spectra at 450–500 nm because this region of the EMS is strongly influenced by the presence and abundance of chlorophyll *a* and *b* (chlorophyll being a large molecule composed of hydrogen, carbon, and oxygen around four central nitrogen atoms and a magnesium atom). In addition, wavelengths in the 450–500-nm range were also used because they did not exhibit correlations with basal area or leaf area index, as did bands in the 600–700-nm range or those straddling the red edge (between 700–750 nm) [15]. First-derivative reflectance from a total of 46 wavelengths of Hyperion and 52 wavelengths of AVIRIS were used in the PLS procedure to extract the factors used to predict canopy N.

The first-derivative reflectance spectra were then input into the PLS procedure in SAS (version 8.2), with the AVIRIS and Hyperion data analyzed separately. Using PLS, one can generate as many factors as dependent variables, thus overfitting the data. We used one-at-a-time cross-validation (dropping each observation and successively recomputing the predictive model) to select the model with the minimum predicted residual sum of squares statistic (PRESS) as having optimum number of factors for the predictive model. Statistical model comparison using randomization [34] was employed to identify the PLS model with the fewest number of factors that was not significantly different from the "best" model at a p-value of 0.10. Following this, we randomized the canopy N data 20 times and reimplemented the PLS procedure to ensure that the PLS predictions were not the result of spurious relationships, after Grossman *et al.* [33]. Finally, PLS models were also developed independently using each of leaf area index (LAI), species composition (percentage plot basal area of each dominant species), and absolute basal area instead of canopy N as dependent variables to demonstrate that associations with the selected image spectra were unique to N concentration.

TABLE III
PERCENT VARIATION ACCOUNTED FOR BY PARTIAL LEAST SQUARES FACTORS FOR HYPERION MODEL

Number of Extracted Factors	Model Effects		Dependent Variables	
	Current	Total	Current	Total
1	15.7	15.7	58.7	58.7
2	9.0	24.7	31.5	90.2
3	7.4	32.1	6.5	96.8
4	8.3	40.4	1.1	97.9

III. RESULTS

For Hyperion, the best PLS model extracted five factors from the spectral data to predict canopy N concentration. However, the model with four factors was not significantly different from the five-factor model and was selected for mapping. The four-factor model accounted for 97.9% of the variation in the N data and 40.4% of the variation in the spectral data (Table III), indicating good prediction of canopy N [Fig. 2(a)] but also that the remaining variation in the spectral data was likely due to factors other than N concentration. For AVIRIS, a three-factor model was identified as having both the minimum number of factors and the lowest PRESS statistic (Table IV), accounting

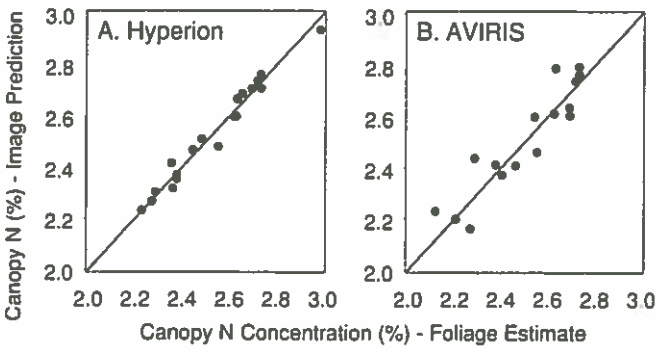

Fig. 2. Image-based predictions of canopy nitrogen concentration versus foliage-based estimates for (A) Hyperion and (B) AVIRIS.

TABLE IV
PERCENT VARIATION ACCOUNTED FOR BY PARTIAL LEAST SQUARES FACTORS FOR AVIRIS MODEL

Number of	Model Effects		Dependent Variables	
Extracted Factors	Current	Total	Current	Total
1	50.0	50.0	29.7	29.7
2	6.8	56.7	51.1	80.8
3	15.6	72.4	4.1	84.9

for 84.9% of the variation in N [Fig. 2(b)] and 72.4% of the variation in the spectral data. None of the implementations of PLS using randomized N data and correct reflectance data yielded models with any number of factors that were significantly different from the null model. This indicated that it was unlikely that the factors and models identified from the PLS analyses of the correct dataset were the result of spurious relationships.

Maps of canopy N concentration derived from PLS (Fig. 3) exhibit similar patterns in the Hyperion and AVIRIS predictions (area of overlap is noted). Hyperion and AVIRIS predictions of canopy N concentration were within 0.25%N for > 70% of the overlap area, with an additional 25% of the overlap area predicted within 0.25% to 0.5%N of each other. Predictions for the field plots in the overlap area also matched closely (Fig. 4). All of the predictions were within 0.25%N of the leaf-based estimates, which is not surprising due to the high degree of explanation from the PLS model.

No statistically significant models could be developed using PLS to predict LAI, basal area, or composition as a function of the selected wavebands. This indicated that the relationships between N concentration and the first-derivative wavebands that we used were due to variations in canopy N (or a related factor), but not LAI, composition or basal area. Simple correlation analyses also indicated that of the first-derivative wavebands that correlated strongest with canopy N concentration (499, 1175, and 1508 nm for Hyperion and 1513, 1642, and 2349 nm for AVIRIS), only 1508 nm (Hyperion) and 1642 nm (AVIRIS) correlated significantly with LAI (but less so than N with the same bands), and none correlated significantly with composition variables or basal area. In fact, few of the wavebands used in the PLS analyses correlated significantly with LAI, basal area or composition, but many correlated with canopy N concentration.

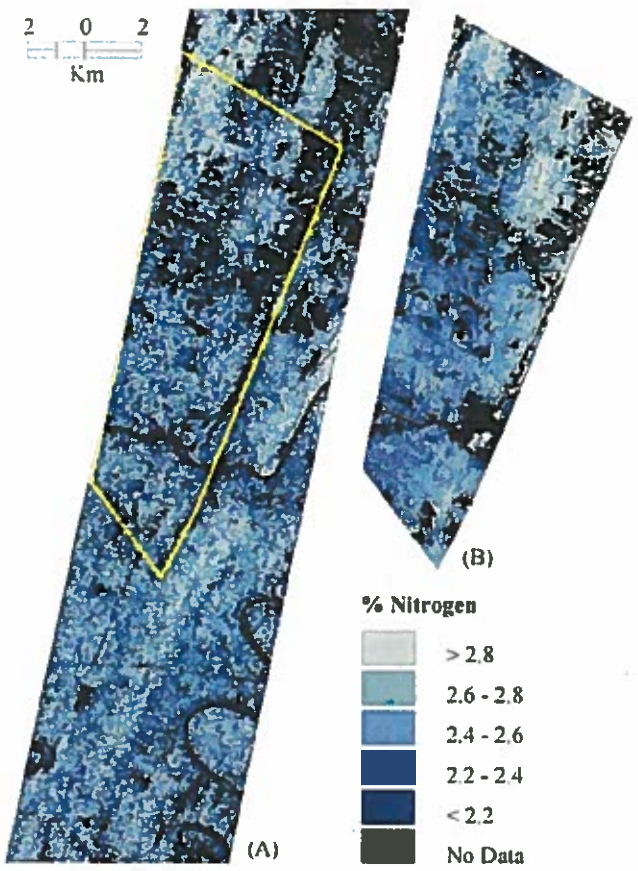

Fig. 3. Maps of predicted canopy nitrogen concentration using Hyperion (A) and AVIRIS (B). Inset area on A indicates area of overlap between Hyperion and AVIRIS. Clouds and nonforest areas are masked out for each date.

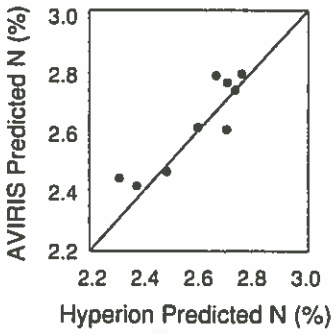

Fig. 4. Comparison of image-derived predictions of canopy nitrogen concentration for Hyperion and AVIRIS for plots in the area of overlap in Fig. 3.

IV. DISCUSSION

The analyses indicate that partial least squares regression can be used with both Hyperion and AVIRIS to develop predictions of canopy nitrogen concentration. The data range for the maps generated by the predictive models fit the expected data range for the study area (1.8% to 3.2%) with very few predictions outside this data range. Although the model fit was better for Hyperion than AVIRIS, this was accomplished using a larger number of factors (four rather than three). In addition,

maps of the AVIRIS predictions were less speckled than Hyperion, which may be due to higher signal to noise ratio in the AVIRIS data [35]. Indeed, Smith and Curran [36] indicated that early 90's AVIRIS data (with SNR comparable to Hyperion) was merely adequate for estimating foliar biochemical concentrations, while the high SNR AVIRIS data from after 1995 was more than adequate. Thus, the PLS factors accounted for more variation in the predictor (spectral) data from AVIRIS than Hyperion (72.4% for AVIRIS to 40.4% for Hyperion), suggesting a more direct relationship between spectra and canopy N in the AVIRIS spectra. This is also an indication of noisiness in the Hyperion data, i.e., much of the variation in the selected wavelengths was due to factors other than N absorption in canopy foliage. Nevertheless, the results indicate that hyperspectral data from both sensors can be used to estimate the spatial distribution of canopy nitrogen. From an operational perspective, both Hyperion and AVIRIS are suitable to generate predictions within 0.25%N of ground estimates, readily meeting the criteria suggested by Schimel [37] for the accuracy of spatial estimates of N concentration to be used for modeling broad scale impacts of increases in greenhouse gas concentrations, N deposition or other environmental changes. However, because of the nature of the empirical approach and differences between Hyperion and AVIRIS, the results for one sensor are not applicable the other, nor are the results necessarily applicable to other images collected using the same sensor.

The selection of statistical techniques has important implications for the results of any empirical modeling exercise. With PLS regression, one must select the independent variables, but the nature of the method is that it can employ high dimensional predictor data by extracting a small number of factors that account for the correlation/variation in the predictors. Nevertheless, one must still decide whether to use all wavelengths or a subset of wavelengths, and whether to use the raw reflectance spectra or derivative reflectance spectra. We limited our analyses to first-derivative reflectance spectra of wavelengths that had been demonstrated in the literature to be related directly to N absorption features (through chemical bonds) or to chlorophyll a and b which act as additional surrogates for N concentration. This limited the possibility of spurious relationships and also provided a defensible argument for the use of the wavelengths that were selected. By using first-derivative reflectance spectra, the analyses focused on the slope of reflectance spectra, in theory identifying differences related to the magnitude of N-related absorption features. The use of first-derivative spectra also lessened the effects of topographically induced shading, which influences overall reflectance [38] but not the shape of the derived spectral reflectance curve.

Aspects of data processing and analysis may have affected the results. First, the estimates of canopy nitrogen concentration were based on extrapolations from a small number of leaf samples. As with any such study, there was the possibility of measurement error on the ground, as well as errors in compositing the leaf N measurements for a plot based on species abundance. Associated with this was the possibility that variations in canopy closure, LAI, and the spectral mixture of leaves, branches, shade and ground in an image pixel may have confounded predictions generated using the imagery. The forests in the study area are generally mature, even-aged, and have a mostly closed canopy, but variations in reflectance due to factors other than N concentration were certainly present [39]. Nevertheless, we conclude that canopy foliar N was the primary source of variation in the selected wavebands, especially because those bands did not correlate significantly with LAI, basal area or species composition. Finally, image processing procedures can affect the derived spectra used in the analyses. For example, ATREM was designed for use with whiskbroom sensors; as such, the atmospherically corrected reflectances used for the Hyperion analysis have not adequately accounted for "smile" in the pushbroom Hyperion sensor [27], [35], [40] so that there is the increased potential for error in the calibrated Hyperion reflectances compared to the AVIRIS reflectances. However, we expect this to be a minor source of error in the statistical analyses compared to possible estimation/measurement errors or spectral variations due to the structural complexity of the forest canopies.

V. Conclusion

Partial least squares analyses of canopy N concentration with AVIRIS and Hyperion imagery yielded statistically significant predictive models that produced very similar maps of canopy N for the two sensors. Because the predictions of N concentration in the two maps are mostly within 0.25%, we believe that the results from both sensors are relatively robust and that the approach is generally applicable where appropriate canopy N data are available. Although a generalized analytical methodology may be possible for estimating N concentration using imaging spectroscopy, it is unlikely that anything other than localized empirical methods will yield reasonable results due to fundamental differences among sensors and because spectral variations due to canopy structure and species composition between study areas may be substantial. Nevertheless, this research demonstrates the practical utility of EO-1 Hyperion, the first orbital imaging spectrometer. In addition, the potential in the future for widely available hyperspectral imagery will mean that scientists and managers will be able to make spatial estimates of a variable critical to understanding the functioning of ecosystems. Further analyses should be conducted to determine the intercomparability of models developed for multiple study areas and using multiple sensors.

Acknowledgment

Thanks to G. Frech, C. Kingdon, K. Lott, C. Baros, and J. Thompson for field and laboratory support. Thanks also to S. Seagle (Appalachian Laboratory) his contributions to and support of this research. The authors thank P. Curran and two anonymous reviewers for insightful comments and recommendations that improved this manuscript. This is scientific contribution number 3617 of the Appalachian Laboratory, University of Maryland Center for Environmental Science.

References

[1] D. L. Peterson, J. D. Aber, P. A. Matson, D. H. Card, N. Swanberg, C. Wessman, and M. Spanner, "Remote sensing of forest canopy and leaf biochemical contents," *Remote Sens. Environ.*, vol. 24, pp. 85–108, 1988.

[2] C. A. Wessman, J. D. Aber, D. L. Peterson, and J. M. Melillo, "Remote sensing of canopy chemistry and nitrogen cycling in temperate forest ecosystems," *Nature*, vol. 335, pp. 154–156, 1988.
[3] C. A. Wessman, J. D. Aber, and D. L. Peterson, "An evaluation of imaging spectrometry for estimating forest canopy chemistry," *Int. J. Remote Sens.*, vol. 10, pp. 1293–1316, 1989.
[4] P. M. Treitz, "Hyperspectral remote sensing for estimating biophysical parameters of forest ecosystems," *Progress Phys. Geography*, vol. 23, pp. 359–390, 1999.
[5] P. J. Curran, "Remote sensing of foliar chemistry," *Remote Sens. Environ.*, vol. 30, pp. 271–278, 1989.
[6] M. L. Smith, S. V. Ollinger, M. E. Martin, J. D. Aber, R. A. Hallett, and C. J. Goodale, "Direct estimation of aboveground productivity through hyperspectral remote sensing of canopy nitrogen," *Ecolog. Appl.*, vol. 12, 2002.
[7] M. E. Martin and J. D. Aber, "High spectral resolution remote sensing of forest canopy lignin, nitrogen, and ecosystem processes," *Ecolog. Appl.*, vol. 7, pp. 431–443, 1997.
[8] S. V. Ollinger, M. L. Smith, M. E. Martin, R. A. Hallett, C. L. Goodale, and J. D. Aber, "Regional variation in foliar chemistry and N cycling among forests of diverse history and composition," *Ecology*, vol. 83, pp. 339–355, 2002.
[9] J. D. Aber and J. M. Melillo, "Nitrogen immobilization in decaying hardwood leaf litter as a function of initial nitrogen and lignin content," *Can. J. Botany*, vol. 60, pp. 2263–2269, 1982.
[10] W. T. Peterjohn and D. L. Correll, "Nutrient dynamics in an agricultural watershed: Observations on the role of a riparian forest," *Ecology*, vol. 65, pp. 1466–1475, 1984.
[11] P. M. Vitousek, J. D. Aber, R. W. Howarth, G. E. Likens, P. A. Matson, D. W. Schindler, W. H. Schlesinger, and D. G. Tilman, "Human alteration of the global nitrogen cycle: Sources and consequences," *Ecolog. Appl.*, vol. 7, pp. 737–750, 1997.
[12] A. H. Magill, J. D. Aber, J. J. Hendricks, R. D. Bowden, J. M. Melillo, and P. A. Steudler, "Biogeochemical response of forest ecosystems to simulated chronic nitrogen deposition," *Ecolog. Appl.*, vol. 7, pp. 402–415, 1997.
[13] J. M. Melillo, A. D. McGuire, D. W. Kicklighter, B. Moore, C. J. Vorosmarty, and A. L. Schloss, "Global climate-change and terrestrial net primary production," *Nature*, vol. 363, pp. 234–240, 1993.
[14] J. D. Aber, "Nitrogen cycling and nitrogen saturation in temperate forest ecosystems," *Trends in Ecology and Evolution*, vol. 7, pp. 220–224, 1992.
[15] J. A. Kupiec and P. J. Curran, "Decoupling effects of the canopy and foliar biochemicals in AVIRIS spectra," *Int. J. Remote Sens.*, vol. 16, pp. 1731–1739, 1995.
[16] J. P. Gastellu-Etchegorry, F. Zagolski, E. Mougin, G. Marty, and G. Giordano, "An assessment of canopy chemistry with AVIRIS—A case-study in the Landes Forest, South-West France," *Int. J. Remote Sens.*, vol. 16, pp. 487–501, 1995.
[17] M. E. Martin, M. L. Smith, S. V. Ollinger, R. A. Hallett, C. L. Goodale, and J. D. Aber, "Applying AVIRIS at the sub-regional scale: Forest productivity and nitrogen and cation cycling," *Proc. Summaries of the 8th JPL Airborne Earth Science Workshop*, pp. 275–279, 1999.
[18] F. Zagolski, V. Pinel, J. Romier, D. Alcayde, J. Fontanari, J. P. Gastellu-Etchegorry, G. Giordano, G. Marty, E. Mougin, and R. Joffre, "Forest canopy chemistry with high spectral resolution remote sensing," *Int. J. Remote Sens.*, vol. 17, pp. 1107–1128, 1996.
[19] P. Matson, L. Johnson, C. Billow, J. Miller, and R. L. Pu, "Seasonal patterns and remote spectral estimation of canopy chemistry across the Oregon transect," *Ecolog. Appl.*, vol. 4, pp. 280–298, 1994.
[20] D. L. Peterson and G. S. Hubbard, "Scientific issues and potential remote-sensing requirements for plant biochemical content," *J. Imaging Sci. Technol.*, vol. 36, pp. 446–456, 1992.
[21] R. F. Kokaly and R. N. Clark, "Spectroscopic determination of leaf biochemistry using band-depth analysis of absorption features and stepwise multiple linear regression," *Remote Sens. Environ.*, vol. 67, pp. 267–287, 1999.
[22] J. Mash, *The Land of the Living*. Cumberland, MD: Commercial, 1996.
[23] P. A. Townsend, R. A. Chastain, C. C. Kingdon, and S. W. Seagle, "Remote sensing of forest structure using multi-temporal, multi-sensor orbital SAR," in *Proc. ASPRS Ann. Conf.*, Washington, DC, 2000.
[24] P. A. Townsend and S. J. Walsh, "Remote sensing of forested wetlands: Application of multitemporal and multispectral satellite imagery to determine plant community composition and structure in Southeastern USA," *Plant Ecol.*, vol. 157, pp. 129–149, 2001.
[25] P. M. Rich, J. Chen, R. Sulatycki, R. Vashisht, and W. S. Wachspress, "Calculation of leaf area index and other canopy indices from gap fraction: A manual for the LAICALC software," Kansas Applied Remote Sensing Program, Lawrence, KS, 1995.
[26] D. A. Vieglais and P. M. Rich, *Hemiview Analysis of Hemispherical Imagery (Version 2.1)*. Cambridge, UK: Helios Environmental Modeling Inst. and Delta-T Devices, 1997.
[27] S. G. Ungar, J. S. Pearlman, J. Mendenhall, and D. Reuter, "Overview of the Earth Observing 1 (EO-1) mission," *IEEE Trans. Geosci. Remote Sensing*, vol. 41, pp. 1149–1159, June 2003.
[28] R. E. Kennedy, W. B. Cohen, and G. Takao, "Empirical methods to compensate for a view-angle-dependent brightness gradient in AVIRIS imagery," *Remote Sens. Environ.*, vol. 62, pp. 277–291, 1997.
[29] B. C. Gao, K. B. Heidebrecht, and A. F. H. Goetz, "Derivation of scaled surface reflectances from AVIRIS data," *Remote Sens. Environ.*, vol. 44, pp. 165–178, 1993.
[30] R. F. Kokaly, "Investigating a physical basis for spectroscopic estimates of leaf nitrogen concentration," *Remote Sens. Environ.*, vol. 75, pp. 153–161, 2001.
[31] K. L. Bolster, M. E. Martin, and J. D. Aber, "Determination of carbon fraction and nitrogen concentration in tree foliage by near infrared reflectance: A comparison of statistical methods," *Can. J. Forest Res.*, vol. 26, pp. 590–600, 1996.
[32] *SAS/STAT User's Guide, Version Six*, 4th ed., SAS Institute, Inc., Cary, NC, 1989.
[33] Y. L. Grossman, S. L. Ustin, S. Jacquemoud, E. W. Sanderson, G. Schmuck, and J. Verdebout, "Critique of stepwise multiple linear regression for the extraction of leaf biochemistry information from leaf reflectance data," *Remote Sens. Environ.*, vol. 56, pp. 182–193, 1996.
[34] H. van der Voet, "Comparing the predictive accuracy of models using a simple randomization test," *Chemotron. Intell. Lab. Syst.*, vol. 25, pp. 313–323, 1994.
[35] R. O. Green, T. G. Chrien, and B. Pavri, "On-orbit radiometric and spectral calibration characteristics of EO-1 Hyperion derived with an underflight of AVIRIS and *in situ* measurements at Salar de Arizaro, Argentina," *IEEE Trans. Geosci. Remote Sensing*, vol. 41, pp. 1194–1203, June 2003.
[36] G. M. Smith and P. J. Curran, "The signal-to-noise ratio (SNR) required for the estimation of foliar biochemical concentrations," *Int. J. Remote Sens.*, vol. 17, pp. 1031–1058, 1996.
[37] D. L. Schimel, "Terrestrial biogeochemical cycles: Global estimates with remote sensing," *Remote Sens. Environ.*, vol. 51, pp. 49–56, 1995.
[38] P. A. Townsend and J. R. Foster, "Terrain normalization of AVIRIS and Hyperion imagery in forested landscapes," in *Proc. 11th JPL Airborne Earth Science Workshop*, R. O. Green, Ed.. Pasadena, CA, 2002.
[39] J. R. Foster and P. A. Townsend, "Mapping forest composition in the central appalachians using AVIRIS: Effects of topography and phenology," in *Proc. 11th JPL Airborne Earth Science Workshop*, R. O. Green, Ed.. Pasadena, CA, 2002.
[40] A. F. H. Goetz, B. C. Kindel, M. Ferri, and Z. Qu, "HATCH: Results from simulated radiances, AVIRIS and Hyperion," *IEEE Trans. Geosci. Remote Sensing*, vol. 41, pp. 1215–1222, June 2003.
[41] B. Datt, T. R. McVicar, T. G. Van Niel, D. L. B. Jupp, B. Datt, and J. S. Pearlman, "Preprocessing EO-1 Hyperion hyperspectral data to support the application of agricultural indexes," *IEEE Trans. Geosci. Remote Sensing*, vol. 41, pp. 1246–1259, June 2003.

Philip A. Townsend (S'95–A'97) received the B.A. degree from the University of Virginia, Charlottesville, in 1989, and the Ph.D. degree in geography from the University of North Carolina, Chapel Hill, in 1997.

He is currently an Assistant Professor at the Center for Environmental Science, Appalachian Laboratory, University of Maryland, Frostburg. His research interests include the use of multispectral, hyperspectral, and SAR remote sensing to map and model forest ecosystem structure and functioning at the watershed and larger scales.

Jane R. Foster received the B.A. degree in biology from Yale University, New Haven, CT, and the M.S. degree in forest science from the Yale School of Forestry and Environmental Studies, New Haven, CT, in 1996 and 2000, respectively.

She has been with the Center for Environmental Science, Appalachian Laboratory, University of Maryland, Frostburg, since 2000, where she specializes in remote sensing applications to forest ecology.

Robert A. Chastain, Jr. received the B.A. from Florida State University, Tallahassee, in 1988, and the M.A. degree in geography from the University of North Carolina, Chapel Hill, in 1995. He is currently pursuing the Ph.D. degree in marine, estuarine and environmental sciences from the University of Maryland, College Park.

His research focuses on forest understory dynamics, remote sensing of forest structure and composition, and modeling forest change across landscapes.

William S. Currie received the B.S. degree in physics from Brown University, Providence, in 1983, the M.S. degree in environmental science from the University of Virginia, Charlottesville, in 1992, and the Ph.D. degree from the Institute for the Study of Earth, Oceans and Space, University of New Hampshire, Durham, in 1995.

He is currently an Assistant Professor at the Center for Environmental Science, Appalachian Laboratory, University of Maryland, Frostburg. He has been a Postdoctoral Scholar at the Ecosystems Center, Woods Hole, MA. His research concerns modeling the biogeochemistry of terrestrial ecosystems at multiple scales, including carbon cycling, nutrient cycling, and energetics.